Supporting Information

Functionalized silver nanoparticles for SERS amplification with enhanced reproducibility and for ultrasensitive optical fiber sensor environmental and biochemical assay

Nguyen Tran Truc Phuong [a,b], Vinh Quang Dang [a,b], Le Van Hieu [a,b], Ta Ngoc Bach [c], Bui Xuan Khuyen [c], Hanh Kieu Thi Ta [a,b], Heongkyu Ju [d], Bach Thang Phan[b,e], Nhu Hoa Thi Tran [a,b*]

[a]Faculty of Materials Science and Technology, University of Science, Ho Chi Minh City, Vietnam

[b]Vietnam National University, Ho Chi Minh City, Vietnam

[c]Institute of Materials Science, Vietnam Academy of Science and Technology, Hanoi, Vietnam

[d]Department of Physics, Gachon University, Seongnam, Gyeonggi-do 13120, Republic of Korea

[e]Center for Innovative Materials and Architectures (INOMAR), HoChiMinh City, Viet Nam

*To whom correspondence should be addressed: ttnhoa@hcmus.edu.vn

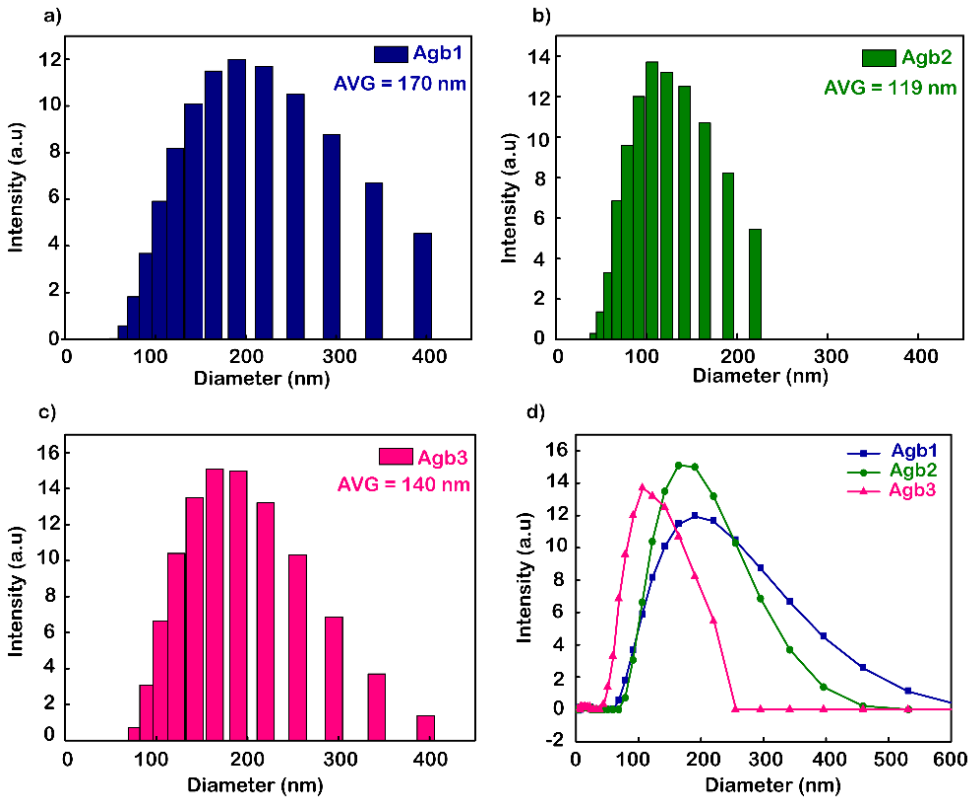

Fig. S1. Dynamic light scattering (DLS) showing the size distribution of Ag NPs synthesized. a) 100 mg PVP (Agb1), b) 90 mg PVP (Agb2), c) 80 mg PVP (Agb3), d) DLS spectrum of Agb1, Agb2, Agb3.

The results from the DLS spectrum (Fig. S1) show that Agb2 has the most uniform particle size distribution, the average size of the particles is calculated as 119 nm. whereas Agb1 and Agb3 have larger mean sizes of 170, and 140 nm, respectively. This contributes to demonstrating that the particle size decreases with increasing PVP mass during synthesis. However, when PVP increased to a certain level, it will impede corrosion of Na_2S leading to the particle size increase.

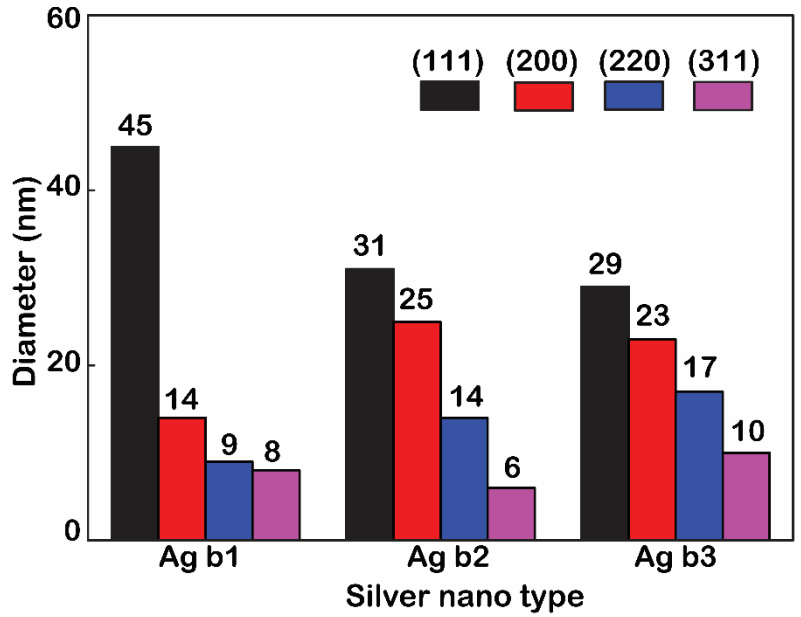

Fig. S2. The crystalline size of Agb1, Agb2, and Agb3 is calculated from the formula Scherrer.

Fig. S2 shows the crystalline size calculated by Scherrer's formula of the characteristic crystal directions of silver. Based on the developmental distribution of the lattice faces, some shape properties can be obtained. Agb1 has crystals that develop in the (111) orientation that are too dominant compared to other crystals, so the Ag NPs shape will not be balanced but deflected in the (111) orientation[1]. For Agb2 and Agb3 different crystals grow more evenly although directional crystals (111) still dominate. So, Ag NPs in those structures (Agb2 and Agb3) will have the shape of uniform faces [2]

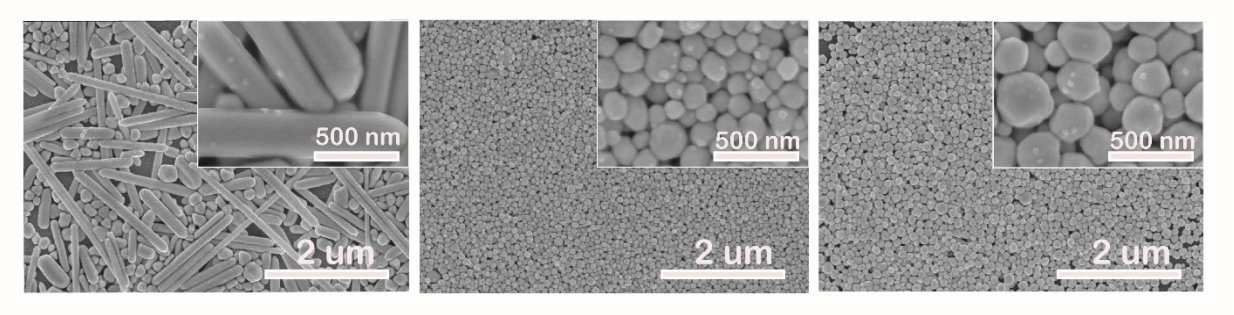

Fig. S3. FESEM image of Agb1 (100 mg PVP), Agb2 (90 mg PVP), Agb3 (80 mg PVP) samples. a), d) Agb1; b), e) Agb2; c), f) Agb3.

In the FESEM results (Fig. S3), Agb1 is proven to contain a mixture of Ag NPs with many different shapes and sizes such as rod, triangular, and cube, ... opposite to Agb2 and Agb3 consist of only spherical silver nanoparticles. The size particle diameters of Agb2 and Agb3 are 80 nm and 120 nm, respectively. This result is completely consistent with the conclusion from the UV-vis spectrum and XRD data (Fig. 1). The reason that Agb1 has many different shapes is that in this method EG was not only the solvent but also the reductant of Ag^+ into Ag [1]. After being formed, the Ag nuclei seed was grown by the twinned and multi-twinned mechanism which was the binding of the twinned particles at the lowest-energy facets in (111) surface [3]. However, the Ag NPs formed by this principle was either nanorods or irregular morphologies [4,5]. To prevent the production of undesirable morphologies, sulfide was added as the etchant to support the formation of Ag NPs because the rods were rapidly dissolved and formed the cubic particles again [6]. When the amount of PVP is too much, in addition to the function of stabilizing Ag NPs, it also interferes with the corrosion of Na_2S leading to rod formation and many different morphologies.

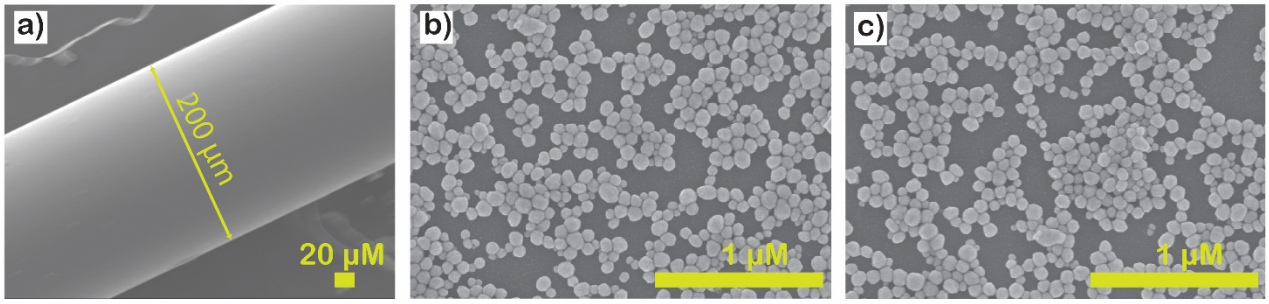

Fig. S4. FESEM images of a) fiber core surface, b) AgNPs on the glass substrate at incubation time 1 h, and Ag NPs on the fiber at incubation time 1 h.

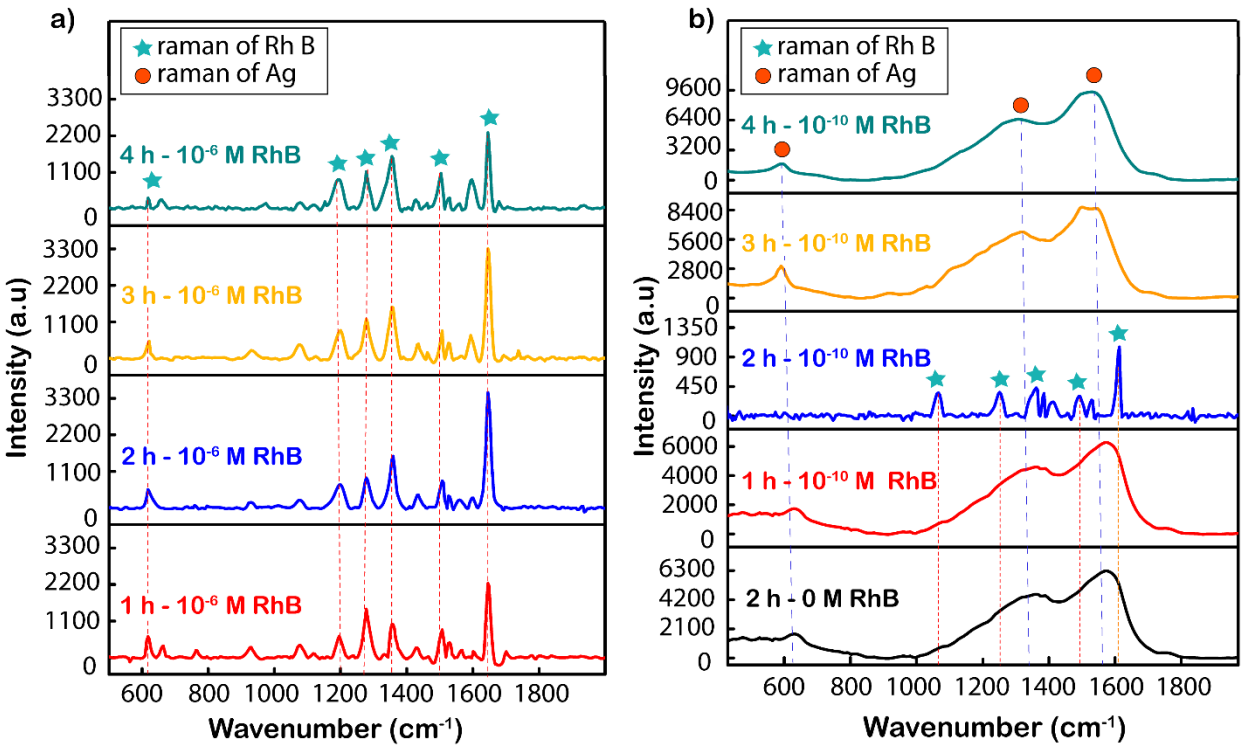

Fig. S5. Surface Raman enhancement spectrum (SERS) of Agb2 with immersion time 1, 2, 3 h. a) RhB concentration at 10^{-6} M, b) RhB concentration at 10^{-10} M.

In the immersion time of Ag NPs on glass, Ag-SERS substrates are used to make substrate that enhances the Raman signal of RhB. The results from the time-enhanced Raman spectrum of 10^{-6} M RhB (Fig. S5a) concentration can see the characteristic oscillation peaks at wavenumbers 1648, 1508, 1357, 1280, and 1192 cm^{-1} respectively. The signal intensity reached the highest value for Ag NPs films with soaking times of 2 and 3 h. Next, the same series of samples were also used to investigate RhB concentrations of 10^{-10} M (Fig. S5b). The Ag NPs membrane is soaked for 1, and 3 h no longer recorded Raman signal of RhB instead of the silver peak with very high intensity [7]. This can be explained by the distribution and spacing of Ag NPs on the glass surface when immersed in a silver solution at different times. When the Ag NPs are too far apart or too close to each other, the fluorescence intensity will increase, and the Raman signal will weaken. At a very close distance from the surface of the NPs, the fluorescence intensity is almost extinguished, and the Raman signal is dominant. As this distance increases, the Raman signal will be strongly attenuated [8].

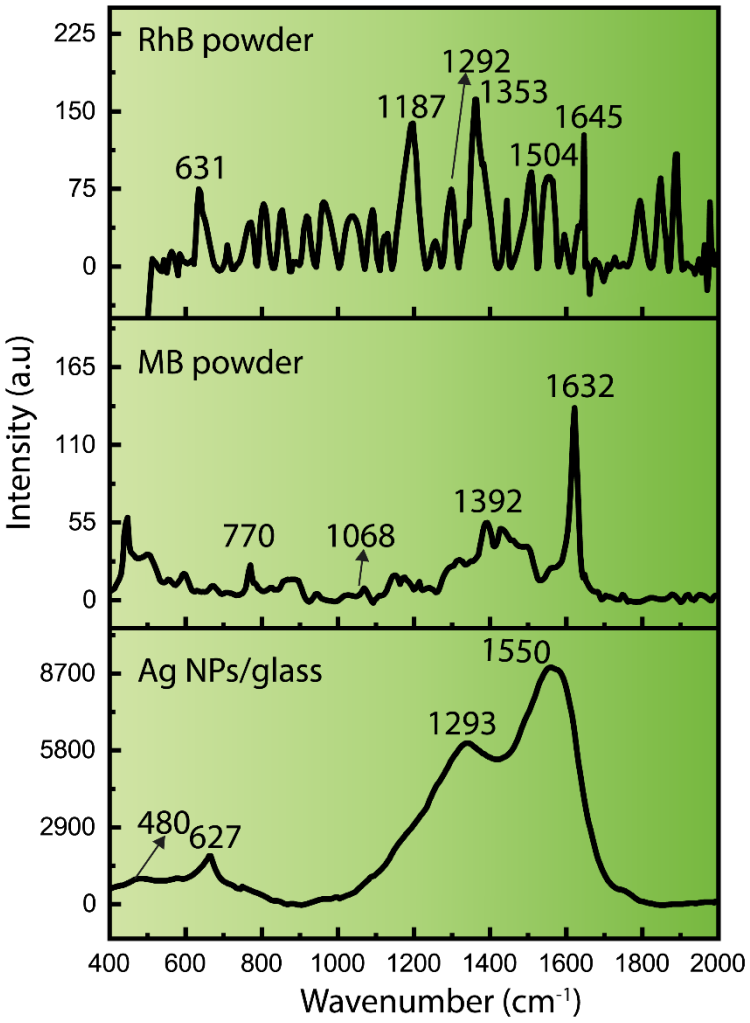

Fig. S6. Raman spectra of rhB powder, MB powder, and Ag NPs/glass substrates.

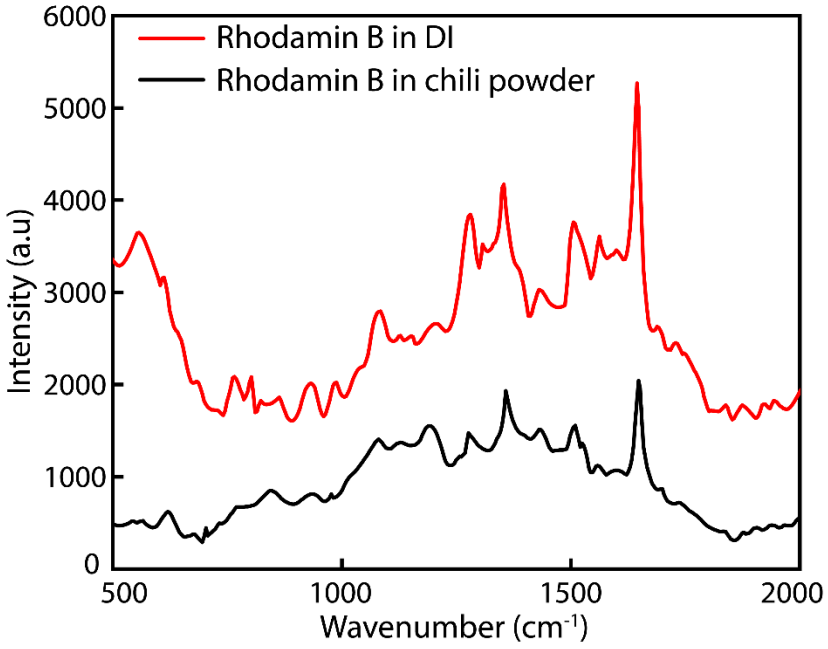

Fig. S7. Raman spectra of rhB in chili powder at a concentration of 2.4 × 10^{-7} g/g (10 ml of rhB 10^{-8} M in 0.2 g of chili powder) and rhB in DI at a concentration of 10^{-8} M on AgNPs/glass substrate.

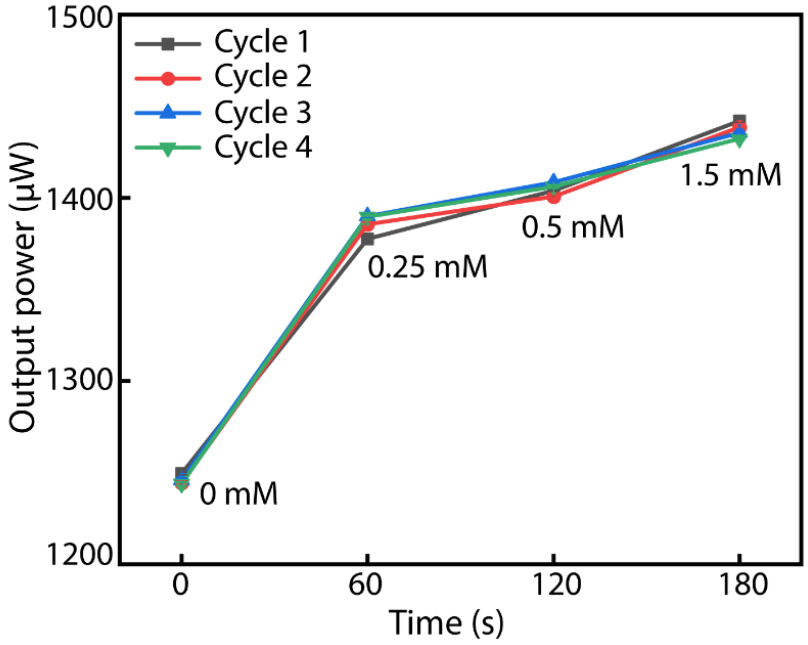

Fig. S8. The reproducibility of the optical fiber sensor was investigated through 4 recycles in the concentration range from 0 to 1.5 mM.

References

[1] J.G. Allpress,, J. V. Sanders, Surf. Sci. 7 (1967) 1–25.

[2] Y. Sun,, Y. Yin,, B.T. Mayers,, T. Herricks,, Y. Xia, Chem. Mater. 14(11) (2002) 4736–45. 10.1021/cm020587b.

[3] Y. Sun,, Y. Xia, Science (80-.). 298 (2002) 2176–9.

[4] Q. Zhang,, W. Li,, L.P. Wen,, J. Chen,, Y. Xia, Chem. - A Eur. J. 16(33) (2010) 10234–9. 10.1002/chem.201000341.

[5] Y. Sun,, B. Mayers,, Y. Xia, Adv. Mater. 15 (2003) 641–6.

[6] A.R. Siekkinen,, J.M. McLellan,, J. Chen,, Y. Xia, Chem. Phys. Lett. 432 (2006) 491–6.

[7] A.J. Kora,, J. Arunachalam, J. Nanomater. 2012 (2012). 10.1155/2012/869765.

[8] K. Vasilev,, W. Knoll,, M. Kreiter, J. Chem. Phys. 120(7) (2004) 3439–45. 10.1063/1.1640341.